Layer Concept Relative to Hypersonic Boundary Layer Stability," Rept. 66-C-192, 1966, Research and Development Center, General Electric Co., Schenectady, N. Y.

[20] Softley, E. J., Graber, B. C., and Zempel, R. E., "Experimental Observation of Transition of the Hypersonic Boundary Layer," *AIAA Journal*, Vol. 7, No. 2, Feb. 1969, pp. 257–263.

[21] Spangenberg, W. G. and Rowland, W. R., "Optical Study of Boundary-Layer Transition Processes in a Supersonic Air Stream," *The Physics of Fluids*, Vol. 3, No. 5, 1960.

[22] Klebanoff, P. S. and Tidstrom, K. D., "Evolution of Amplified Waves Leading to Transition in a Boundary Layer with Zero Pressure Gradient." TN-D-195, 1959, NASA.

[23] Schubauer, G. B. and Klebanoff, P. S., "Contributions on the Mechanics of Boundary Layer Transition." Rept. 1289, 1956, NACA.

[24] Emmons, H. W., "The Laminar-Turbulent Transition in a Boundary Layer—Part I," *Journal of the Aeronautical Sciences*, Vol. 18, No. 7, July 1951.

[25] Pate, S. R. and Schueler, C. J., "Radiated Aerodynamic Noise Effects on Boundary Layer Transition in Supersonic and Hypersonic Wind Tunnels," *AIAA Journal*, Vol. 7, No. 3, March 1969, pp. 450–477.

[26] Morkovin, M. V., "Critical Evaluation of Transition from Laminar Turbulent Shear Layers with Emphasis on Hypersonically Traveling Bodies," AFFDL-TR-68-149, 1968, Air Force Flight Dynamics Lab., Wright-Patterson Air Force Base, Ohio.

[27] Mack, L. M., "Boundary Layer Stability Theory in Incompressible and Compressible Flow," von Kármán Institute Notes on Mechanics of Boundary Layer Transition, Jan. 1968, Brussels, Belgium; also available as a series of JPL internal reports).

[28] James, C. S., "Observations of Turbulent Burst Geometry and Growth in Supersonic Flow," TN-4235, 1958, NACA.

[29] Kendall, J. M., Jr., "Supersonic Boundary Layer Transition Studies," *JPL Space Programs Summary 37-62*, Vol. III, p. 43; also "J.P.L. Experimental Investigations," presented at Transition Specialists Workshop, Aerospace Corp., San Bernardino, Calif., Nov. 3–5, 1971.

JUNE 1972 AIAA JOURNAL VOL. 10, NO. 6

Hypersonic Transitional Boundary Layers

F. K. OWEN* AND C. C. HORSTMAN†
NASA Ames Research Center, Moffett Field, Calif.

Surface thin film gages have been used to determine the extent of the transition region, intermittency distribution, and disturbance convection velocities in the boundary layer on a sharp 5° half angle cone at $M_\infty = 7.4$ in the Ames 3.5-ft Hypersonic Wind Tunnel. In addition, extensive hot wire space-time correlation measurements have been obtained in the wind-tunnel freestream and in the transitional hypersonic boundary layer on a cone-ogive-cylinder in the same facility. Disturbance convection velocities have been obtained from the longitudinal cross correlation measurements as a function of fluctuation scale and distance from the wall. The results of normal cross correlation measurements are also discussed.

Nomenclature

f = frequency
M = Mach number
p = pressure
Re = Reynolds number
t = time
T = temperature
U = velocity
V' = rms voltage fluctuations
x = distance from model cone apex, along model centerline
Δx = separation distance in x direction
y = distance normal to model surface
z = lateral distance around model
α = disturbance inclination angle
γ = intermittency
δ = boundary-layer thickness determined from Pitot pressure profiles
λ = turbulence scale, $U/2\pi f$

Subscripts

c = convection
e = boundary-layer edge
l = local
o = total
w = wall
∞ = freestream

Received November 5, 1971; revision received January 31, 1972.
Index categories: Boundary-Layer Stability and Transition; Supersonic and Hypersonic Flow.

* NRC Postdoctoral Research Associate.
† Research Scientist. Associate Fellow AIAA.

Introduction

IN spite of the extensive experimental and analytical work which has been conducted in supersonic and hypersonic transitional boundary layers in recent years, there is still much speculation regarding the detailed structure of and mechanisms influencing boundary-layer transition.

Morkovin[1] and Laufer[2] have pointed out that, at high freestream Mach numbers, the sound field which radiates from the turbulent boundary layers on the wind tunnel walls is a major source of freestream disturbances and must be considered in all transition experiments. Recently Pate and Schueler[3] have shown that the effects of aerodynamic noise on boundary-layer transition may be related to a number of wind-tunnel parameters including Mach number and unit Reynolds number. However, the conclusions of Pate and Schueler cannot be extended to all wind-tunnel transition data. For example, the transition data of Mateer and Larson[4] show little unit Reynolds number dependence which would not be expected if the effects of aerodynamic noise were dominant. In particular, noise cannot explain the unit Reynolds number effect observed in the ballistic range experiments of Potter[5] where, in the absence of significant freestream disturbances the variation of transition Reynolds number with unit Reynolds number was comparable to those observed in noise-contaminated wind tunnels. It is apparent that more data are needed to determine the effect of freestream disturbances on boundary-layer transition.

A better understanding of the transition mechanism could be obtained if experiments were designed to obtain a more complete picture of the structure and extent of the transition region

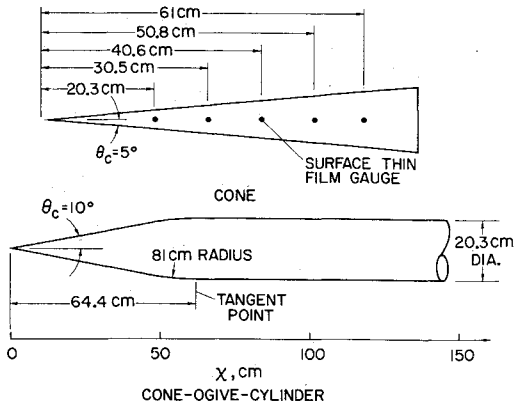

Fig. 1 Test models.

together with fluctuation measurements in the freestream rather than the mere determination of a single transition "point" from mean surface measurements, which has usually been the case. Indeed Laufer[6] has pointed out the general failure of experimenters to exploit the advantages of hot wire anemometry for fluctuation measurements. Consequently, very little is known about the structure of hypersonic transitional boundary layers.

Since turbulent flows vary not only in time but also in space, their investigation must involve an examination of both the spatial and temporal statistical structure. Space-time correlations can contribute to this study since they give evidence of the heredity and structure of turbulence, as well as the convection velocities of the vorticity and entropy modes relative to the average mass transport velocities. Such measurements have been made in incompressible turbulent boundary layers (e.g., Favre et al.[7]) but, to the authors' knowledge, no such measurements have been reported in hypersonic transitional boundary layers.

The purpose of this investigation was to provide detailed measurements of the structure of hypersonic transitional boundary layers. Data on the intermittency distribution, disturbance convection velocities, and extent of the transition region are presented. Extensive hot wire correlation measurements are also presented. Freestream fluctuation measurements have also been made in an attempt to determine the influence of freestream disturbance level on boundary-layer transition.

Experimental Details

Wind Tunnel

The investigation was conducted in the Ames 3.5-ft Hypersonic Wind Tunnel. In this facility, high-pressure air heated in a pebble-bed heater flows through the 1.067 m-diam test section to low-pressure spheres. Using the nominal Mach 7 contoured nozzle, the test conditions were $T_o = 835°K$, $p_o = 13$–122 atm, $M_\infty = 7.4$ for the 5° half angle cone experiments and $T_o = 667°K$, $p_o = 14$–28 atm, $M_\infty = 7.4$ for the cone-ogive-cylinder experiments. The test core diameter was approximately 0.70 m with axial Mach number gradients less than 0.12/m. The nozzle had an annular injection slot in its subsonic portion through which helium or air was injected to provide thermal insulation between the nozzle wall and the hot airstream.

Test Models

All the surface thin film gage measurements were made on a sharp 5° half angle cone at a wall to freestream temperature ratio of approximately 0.4. Five thin film gages were mounted flush with the model surface at distances between 20.3 and 61 cm from the cone apex. The 5° cone transition experiments were conducted using a quick insert mechanism so that the model was never exposed to the hot airstream for more than 15 sec. Thus changes in wall temperature ratio during the tests were negligible.

The hot wire fluctuation measurements were made in the transitional boundary layer on the cylindrical portion of an axisymmetric 10° sharp cone-ogive-cylinder. This test model was 300 cm long and 20.3 cm in diameter. During a typical one minute test the model wall temperature increased a maximum of 20°K on the cone portion of the model and 5°K on the cylindrical portion. The average wall to freestream temperature ratio was 0.45. Details of the two test models are shown in Fig. 1.

Fluctuation Measurements

The measurements were made with constant temperature anemometer systems. The a.c. component of the hot wire and hot film signals, representing the turbulent fluctuations (see appendix), was recorded on the FM system of a multichannel tape recorder. For the correlation measurements, the signals from two anemometers were recorded simultaneously on two tape recorder channels which had been previously checked for phase differences. The autocorrelation and cross correlation were then obtained by playing back the tapes through an analogue correlator. The filtered correlations were obtained using matched $\frac{1}{3}$ octave filters.

Cross correlation measurements involve the correlation of signals from two spatially separated measuring positions, with varying positive or negative time delay of one signal with respect to the other. Thus if $V_1(x_1, y_1, z_1, 0)$ denotes the signal received at one point at time $t = 0$ and $V_2(x_2, y_2, z_2, t)$ denotes the signal received at a second point at time t their cross correlation may be defined as

$$R(V_1 V_2) = \overline{V_1 V_2}/(\overline{V_1^2})^{1/2}(\overline{V_2^2})^{1/2}$$

The space correlation, which involves the comparison of the instantaneous signal received at two spatially separated points is therefore the cross correlation at zero time delay, while the autocorrelation, which involves the comparison of a signal received at one measuring station with the signal received at the same point at time t, is therefore the cross correlation for zero separation.

The upper frequency limits (−3 db) of the surface hot film and hot wire probe systems, as determined by a standard square-wave technique were found to be 30 kHz and 40 kHz, respectively, at the lowest mass flow rates. This enabled fluctuation scales down to one half of the boundary-layer thickness to be recorded and correlated during the turbulent structure experiments.

Discussion of Results

Transition Measurements

Typical variations of the root mean square thin film voltage fluctuations for a range of unit Reynolds numbers are shown in Fig. 2. The curves clearly show a rise from the laminar to the turbulent level with an intermediate peak. Of particular importance is the fact that three distinct points in the transition

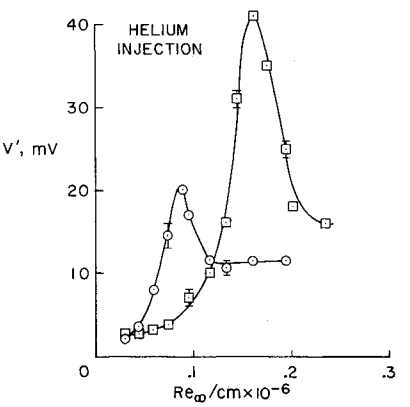

Fig. 2 Surface hot film fluctuation measurements through the transition region on a sharp 5° cone.

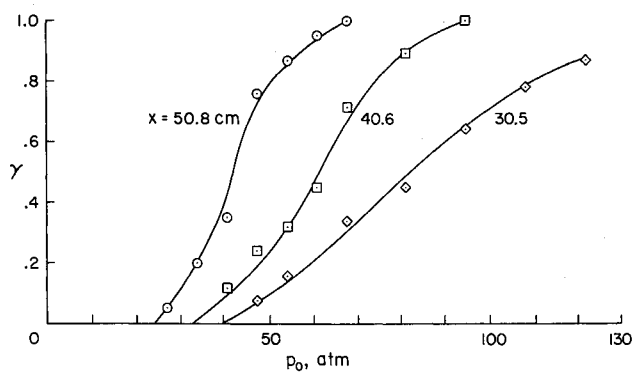

a) Data

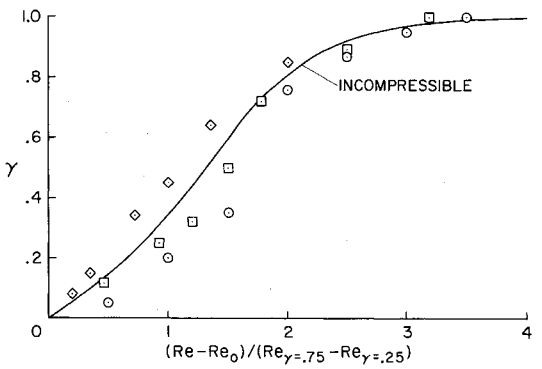

b) Incompressible correlation

Fig. 3 Intermittency distribution through the transitional region on a sharp 5° cone.

region can be accurately located: 1) the start of transition, defined as the point where the rms signal begins to increase from its laminar value, i.e., where intermittency begins; 2) the peak rms signal which coincides with the point where the turbulent burst frequency is a maximum (Owen[8]); and 3) the end of transition.

Intermittency measurements in the transition region, obtained by passing the a.c. components of the hot film signals through a Schmidt trigger circuit, are shown in Figs. 3a and b. There is a close similarity between the intermittency variations in subsonic and hypersonic transitional boundary layers as shown by the

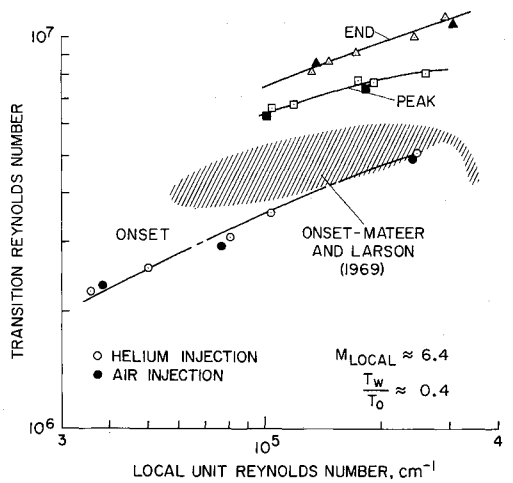

Fig. 4 Variation of transition Reynolds number with unit Reynolds number on a sharp 5° cone.

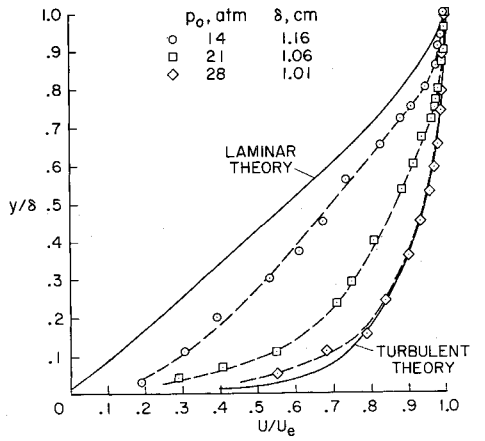

Fig. 5 Velocity profiles through the transition region on the cone-ogive-cylinder, $x = 115$ cm.

good agreement between the present data and the incompressible data of Dhawan and Narashima.[9]

The influence of unit Reynolds number on the magnitude of the transition Reynolds number and the extent of the transition region is presented in Fig. 4. Also shown are previous heat-transfer transition onset data obtained on an "identical" model in the same facility.[4] The onset of transition as defined by the heat transfer measurements is much less sensitive than the thin film gage technique, especially at low unit Reynolds numbers. It is also apparent from Fig. 4 that the heat-transfer technique does not provide consistent transition "point" data since the onset of transition is detected at different values of intermittency depending on the unit Reynolds number.

The authors feel that a lot of the scatter in transition data could be attributed to the inconsistent choice of the transition "point" indicated by the many different techniques which are and have been used. A more complete picture of transition dependence on the various parameters can only be obtained from experiments in which the positions of the beginning and end of transition are accurately determined. It is of interest to note that transition data reported for supersonic and hypersonic flows are not generally based on observations of turbulent spots but rather some macroscopic quantity such as skin friction, heat transfer, or surface Pitot pressure, whose departure from laminar values can be detected only when the intermittency is appreciably greater than zero.

Structure of the Transitional Boundary Layer

Using a hot wire mounted close to the cone-ogive-cylinder model surface ($y/\delta \approx 0.05$) 115 cm from the apex, the beginning and end of transition were determined to occur at tunnel total pressures of 12 and 30 atm, respectively. For reference, the mean velocity profiles obtained from total temperature and Pitot pressure surveys at this location are shown in Fig. 5. The theoretical laminar and turbulent profiles shown in Fig. 5 were obtained from the finite-difference program of Dwyer et al.[10] using actual boundary-layer edge conditions.

Figure 6a shows the autocorrelation of the fluctuation signals midway through transition ($p_o = 21$ atm) at several positions across the boundary layer. It can be seen from these curves that there is a marked variation of energy distribution with frequency across the boundary layer. The power spectral density variations across the boundary layer obtained by Fourier transformation of the autocorrelation curves are shown in Fig. 6b. It can be seen that the maximum fluctuation energy occurs near the boundary-layer edge and decreases as the wall is approached. But, close to the wall there is proportionately more energy associated with the smaller scale disturbances. This "movement" of the relative energy to the smaller scales is believed to be due to the large rates of shear in the wall region. Similar results were also obtained at the two other tunnel total pressures. A

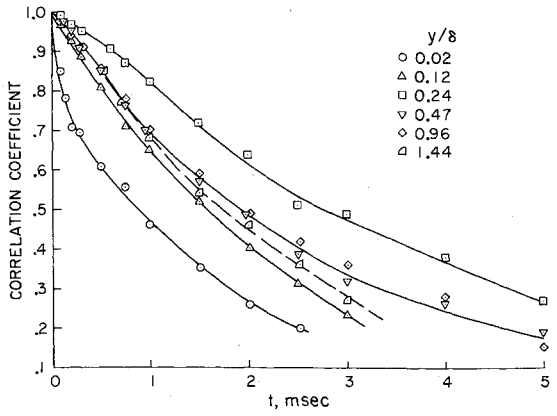

a) Autocorrelation

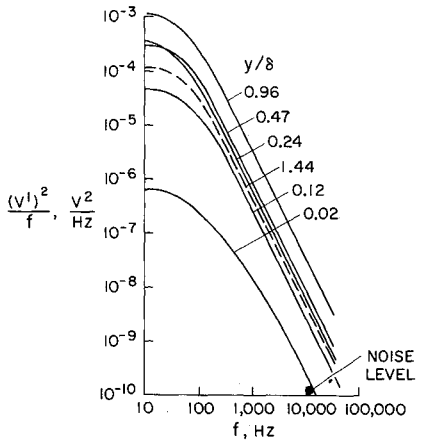

b) Power-spectral-density

Fig. 6 Fluctuating energy distributions through the boundary layer on the cone-ogive-cylinder, $p_o = 21$ atm, $x = 115$ cm.

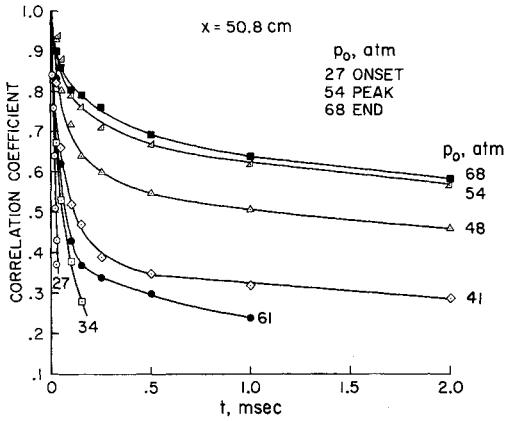

a) Autocorrelation

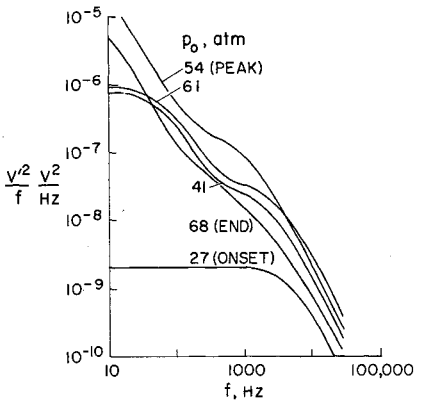

b) Power-spectral-density

Fig. 7 Fluctuating energy distributions through the transition region on the surface of the 5° cone, $x = 50.8$ cm.

typical noise level reading is also indicated on Fig. 6b. It can be seen that even at the higher frequencies the noise is still substantially lower than the signal. At the lower frequencies the noise spectrum was practically undetectable.

The variations of the autocorrelation and power spectral density through the transition region obtained by a surface thin film gage on the cone model are shown in Figs. 7a and b. The very pronounced change in the autocorrelation after the peak (i.e., $p_o = 61$ atm) was observed at all gage locations. Again it can be seen that there are significant changes in power level and distribution with a pronounced energy concentration at the lower frequencies in the transition region. This energy concentration in the transition region is caused by the turbulent bursts passing over the film that change the mean voltage across the film from the laminar to the turbulent level (Owen[8]). The apparent nonmonotonic behavior of the autocorrelation coefficient at 61 atm (after the peak) is due to the intermittency in the fluctuating signal.[8]

The peaks of the cross correlations obtained for various values of wire separation distance represent the autocorrelation in a reference frame moving with the disturbances or the Lagrangian autocorrelation coefficient. It is therefore a measure of the lifetime of the disturbance pattern as it is swept along with the mean flow. The variation of longitudinal correlation coefficient of the total fluctuation field measured at optimum time delay is shown in Fig. 8. The optimum correlation decreases as the space separation increases. In the case of the filtered turbulent field (Fig. 9) the influence of frequency combines with the influence of separation distance and y/δ. When the separation distance is fixed, the higher the frequency the more the optimum correlation coefficient decreases. This indicates that the smaller scale disturbances are decaying at a faster rate than the larger ones. This more rapid decay of the small-scale disturbances explains the selective part played by the longitudinal separation, which reduces their contribution to the correlation coefficient of the total turbulent field as the wire separation increases.

The results of a series of filtered cross correlation measurements at two positions across the boundary layer are shown in Fig. 10. Each cross correlation curve reaches a maximum at some value of the time delay other than zero, clearly indicating the presence of convection. A convection velocity of these

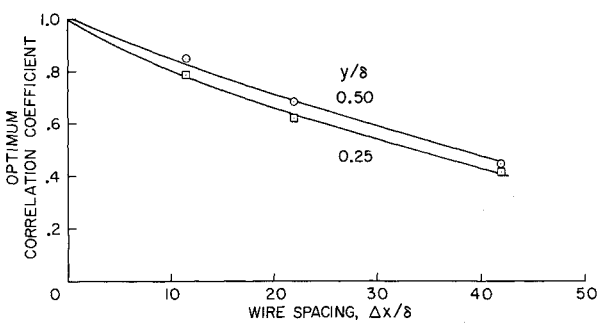

Fig. 8 Optimum space-time correlation coefficients—total turbulent field.

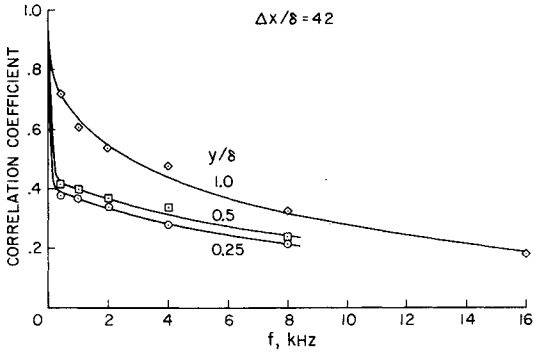

Fig. 9 Optimum space-time correlation coefficients—filtered turbulent field.

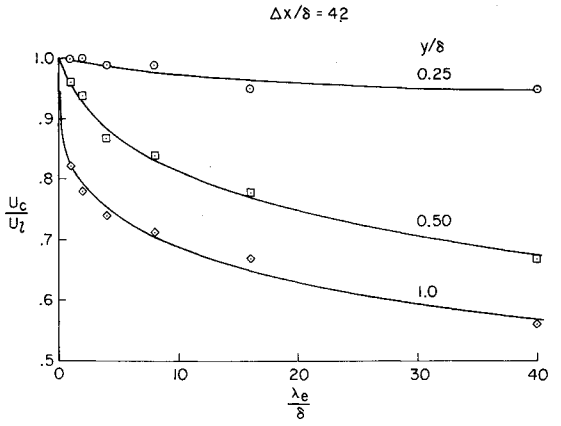

Fig. 11 Effect of disturbance scale on convection velocity.

disturbances may be determined by dividing the separation distance by the time delay at which the maximum of a particular cross correlation occurs. No significant variations of convection velocity with wire spacing were observed. This was also the case for the over-all and other filtered disturbance convection velocities.

The variation of the disturbance convection velocity relative to the local velocity as a function of disturbance scale is shown for one wire spacing in Fig. 11. The ratio, U_c/U_l, tends towards unity as the scale ($\lambda_e = U_e/2\pi f$) decreases. Thus the small-scale fluctuations are convected close to the local mean velocity. However, as the scale increases the more U_c/U_l differs from unity. Near the wall ($y/\delta = 0.25$) the propagation velocities of the disturbances are close to the local velocity whereas they are significantly lower than the local velocity in the outer half of the boundary layer.

The variation of the over-all and filtered convection velocity profiles compared to the mean velocity profile is shown in Fig. 12. At a distance from the wall $y/\delta \approx 0.25$ the convection velocities corresponding to the various scales are close to the local fluid velocity ($U_c \approx 0.72\, U_e$). At greater values of y/δ the differences increase with the scale. In the outer portion of the boundary layer the large-scale disturbances are convected much more slowly than the mean velocity. The transitional surface measurements on the 5° cone (for all disturbance scales) are also shown and can be seen to be in good agreement with the hot wire boundary layer measurements. Since the variations of convection velocity with scale and y/δ are so significant, it is important that they are taken into account in any attempt to relate the frequency spectrum of boundary-layer turbulence to its wave number spectrum.

The values of the cross correlation coefficient have also been determined for various separation distances normal to the wall as a function of the time delay. Figure 13 shows an example of the resulting filtered correlation coefficients. It can be seen that the correlation reaches a maximum value for an optimum time delay t applied to the fluctuations sensed by the probe located farthest from the wall. This optimum time delay, which is a function of the normal separation distance, has been observed previously in an incompressible turbulent boundary layer.[7] These space-time correlations may be interpreted in terms of a disturbance inclination angle to the wall. This angle may be determined by dividing the normal wire separation distance by the product of the observed time delay and the disturbance convection velocity at that point in the boundary layer. The results (Fig. 14) show that this angle is smallest close to the wall, and increases with increasing distance from the wall. Similar results obtained in the fully developed turbulent boundary layer on the same model[11] are represented by the solid curve on Fig. 14.

It is apparent that there is some variation of the propagation angles through the transition region (i.e., as the total pressure changes). Towards the end of transition ($p_o = 28$ atm) these angles approach the fully turbulent values. The propagation angle of about 20° measured close to the wall may be compared with the incompressible experiments of Kline et al.[12] where ejected streaks were observed to leave the wall layer at an angle of about 10°–12°.

Freestream Fluctuation Measurements

Freestream fluctuation measurements have also been made in an attempt to determine if turbulence generation and transition in the model boundary layer are driven by the freestream disturbances. By changing the nozzle wall gas injection it is possible to

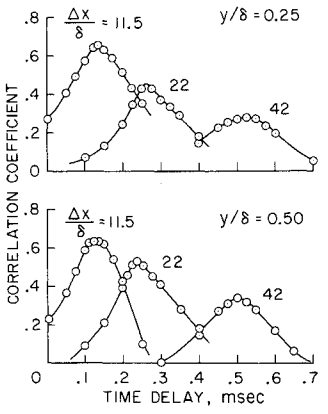

Fig. 10 Examples of filtered space-time correlation coefficients—4 kHz.

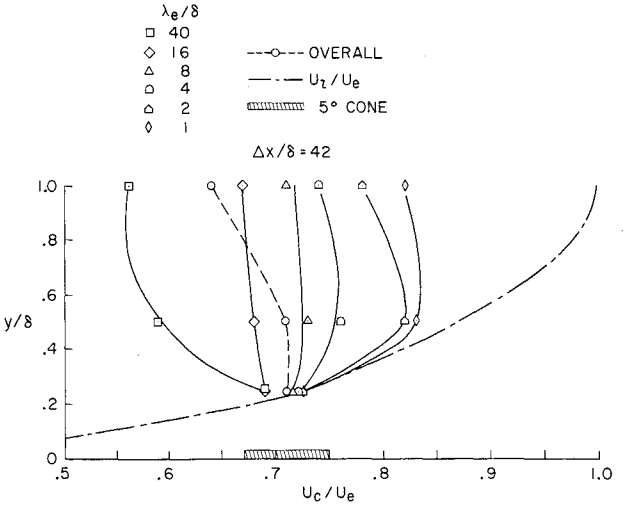

Fig. 12 Distribution of disturbance convection velocities across the boundary layer.

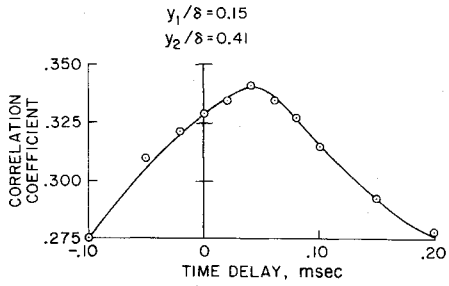

Fig. 13 Filtered transverse space-time correlations—4 kHz.

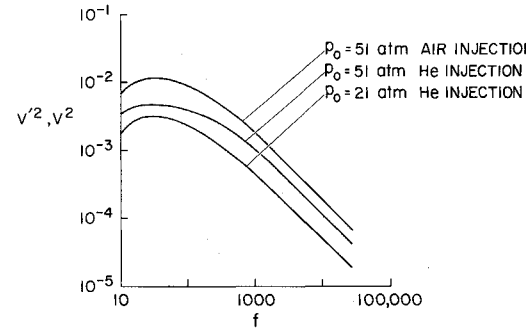

Fig. 15 Freestream power-spectra.

alter the state of the tunnel side wall boundary layer, and consequently, the freestream disturbance level without appreciably changing the unit Reynolds number. Thus it is possible to isolate the effects of changes in the freestream disturbance level without associated changes in unit Reynolds number.

The undisturbed freestream power spectra, obtained without a model in the flow, are presented in Fig. 15 and show comparable changes in magnitude with variations in either unit Reynolds number or tunnel wall boundary layer gas injection. However, transition data obtained with air injection showed no significant differences from the helium injection data (see Fig. 4). If changes in freestream power spectra are important to the transition process one would expect comparable changes in transition location with gas injection as was found for changes in unit Reynolds number. This is not the case.‡

The undisturbed over-all freestream disturbance convection velocity, obtained by cross correlation of the signals from two wires displaced in the stream direction, has also been measured and, as shown in Fig. 16, is in good agreement with the extrapolation of the data taken from Laufer.[13] Also shown are the over-all disturbance convection velocities in the transitional and turbulent boundary layers on the 5° cone and cone-ogive-cylinder models. Although the convection velocities are somewhat faster in the fully turbulent than in the transitional boundary layer, they are all close to the freestream disturbance convection velocity. It is also apparent that the boundary layer and freestream disturbance convection velocities are traveling supersonically relative to the freestream.

The freestream convection velocities did not vary with scale. Since the disturbance velocities in the transitional boundary layer vary significantly with scale and y/δ, it is not obvious that the freestream disturbances are related to the boundary-layer disturbances.

Concluding Remarks

The surface hot film results show that a more complete picture of transition dependence on various parameters could be obtained if the onset and extent of the transition region are accurately and consistently determined. Since changes in freestream disturbance level did not influence the location of boundary-layer transition in the present tests, it is not obvious that differences in freestream power spectra can be blamed for all discrepancies in wind-tunnel transition data.

The longitudinal space-time correlations have shown that there are significant variations in the disturbance convection velocities which depend on both the scale of the disturbance and position in the boundary layer.

Normal space-time correlations have shown that the boundary-layer disturbances are inclined to the wall. This inclination angle varies across the boundary layer. It is smallest close to the wall where the measured angles are in good agreement with previous incompressible measurements.

Appendix: Hot Wire Correlation Measurements

To determine the space-time correlation coefficient in *incompressible* flows we consider two hot wires A and B in the flow at some distance apart in the same perpendicular plane normal to the instantaneous velocity fluctuation (U) which is to be correlated.

Then the voltage signals of the wires A and B are

$$e_A = S_A U_A \quad \text{at time} \quad t$$

and

$$e_B = S_B U_B \quad \text{at time} \quad t'$$

where S_A and S_B are the hot wire sensitivities.

The correlation $\overline{U_A U_B}$ can then be calculated from

$$[\overline{(e_A+e_B)^2} - \overline{(e_A-e_B)^2}]/[\overline{(e_A+e_B)^2} + \overline{(e_A-e_B)^2}] = 2\overline{e_A e_B}/(\overline{e_A^2} + \overline{e_B^2}) \qquad \text{(A1)}$$

provided that the wires are sufficiently alike to assume $S_A = S_B$.

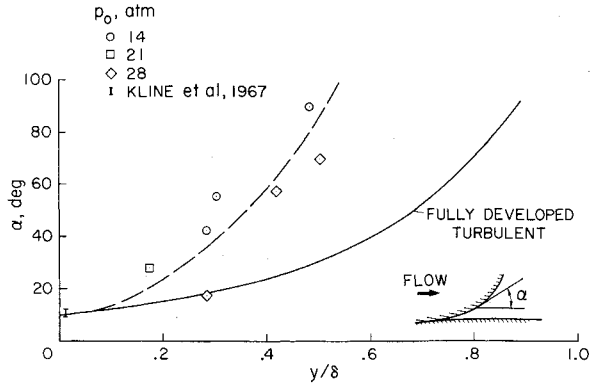

Fig. 14 Disturbance inclination angle.

‡ The authors' recent experiments (to be reported separately) in the Ames 3.5-ft Hypersonic Wind Tunnel and the Langley Variable Density Wind Tunnel confirm this.

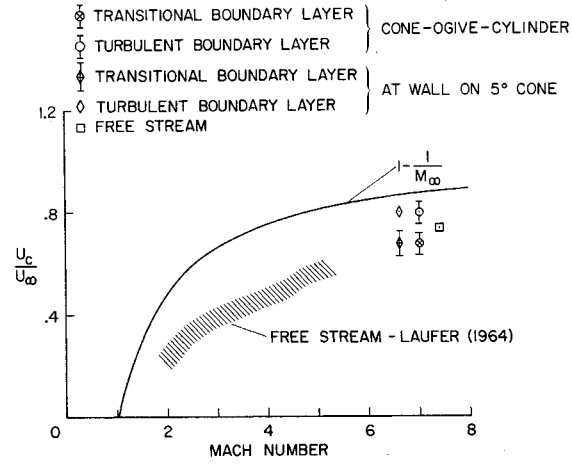

Fig. 16 Comparison of disturbance convection velocities.

Or, if $\overline{e_A^2}$ is adjusted to equal $\overline{e_B^2}$, Eq. (A1) reduces to the correlation coefficient

$$R_{e_A e_B} = \overline{e_A e_B}/e_A' e_B' = \overline{e_A e_B}/\overline{e_A^2} = \overline{e_A e_B}/\overline{e_B^2} \tag{A2}$$

where $'$ denotes root mean square values. In this case it is not necessary to have $S_A = S_B$ since the quantities cancel.

Now in *compressible* flows let m be the instantaneous value of mass flow fluctuation in the direction of the mean flow and θ the temperature fluctuation, then the voltage response of wire A at time t is

$$e_A = \alpha_A m_A + \beta_A \theta_A \tag{A3}$$

and the response of wire B at time t' is

$$e_B = \alpha_B m_B + \beta_B \theta_B \tag{A4}$$

Again if we adjust $\overline{e_A^2} = \overline{e_B^2}$ and substitute (A3) and (A4) in Eq. (A2) we obtain

$$R_{e_A e_B} = \frac{r^2 m_A m_B + r(\overline{m_A \theta_B} + \overline{m_B \theta_A}) + \overline{\theta_A \theta_B} + C}{r_A^2 \overline{m_A^2} + 2 r_A \overline{m_A \theta_A} + \overline{\theta_A^2}} \tag{A5}$$

where

$$r = (\alpha_A \alpha_B/\beta_A \beta_B)^{1/2}, \qquad r_A = \alpha_A/\beta_A$$

and

$$C = [(\alpha_A/\beta_A)^{1/2} - (\alpha_B/\beta_B)^{1/2}] \times [(\alpha_A/\beta_A)^{1/2} \overline{m_A \theta_A} - (\alpha_B/\beta_B)^{1/2} \overline{m_B \theta_A}]$$

However, when the two hot wires A and B are made of the same material and are operated at the same overheat ratio $(\alpha_A/\beta_A)^{1/2} \approx (\alpha_B/\beta_B)^{1/2}$ so that $C \approx 0$ and $r_A^2 = r^2$.

Further, as the overheat ratio tends to zero $\alpha/\beta \to 0$ and Eq. (A5) reduces to the temperature-temperature correlation $(\theta_A \theta_B/\theta_A' \theta_B')$.

At high overheat ratios $\alpha/\beta \to 1.0$ so that when $\theta \ll m$ Eq. (A5) reduces to the mass flux-mass flux correlation $(\overline{m_A m_B}/m_A' m_B')$. Between these two limits a combination of temperature and mass flux correlations will be measured.

In the present experiment the correlation measurements were obtained at high overheat ratios and in the boundary layer where the normal total temperature gradients were much less than the normal mean mass flux gradients. Since the fluctuations scale with their respective mean gradients it can be assumed that $\theta \ll m$ so that the present measurements represent predominantly mass flux space-time correlations.

References

[1] Morkovin, M., "On Supersonic Windtunnels with Low Freestream Disturbances," *Journal of Applied Mechanics*, Vol. 26, 1959, pp. 319–324.

[2] Laufer, J., "Aerodynamic Noise in Supersonic Wind Tunnels," *Journal of Aerospace Sciences*, Vol. 28, Sept. 1961, pp. 685–692.

[3] Pate, S. and Schueler, C., "Effects of Radiated Aerodynamic Noise on Model Boundary Layer Transition in Supersonic and Hypersonic Wind Tunnels," *AIAA Journal*, Vol. 7, No. 3, March 1969, pp. 450–457.

[4] Mateer, G. and Larson, H., "Unusual Boundary-Layer Transition Results on Cones in Hypersonic Flow," *AIAA Journal*, Vol. 7, No. 4, April 1969, pp. 660–664.

[5] Potter, J. L., "Observations on the Influence of Ambient Pressure on Boundary Layer Transition," *AIAA Journal*, Vol. 6, No. 10, Oct. 1968, p. 1907.

[6] Laufer, J., "Thoughts on Compressible Turbulent Boundary Layers," NASA SP-216, 1968, pp. 1–13.

[7] Favre, A., Gaviglio, J., and Dumas, R., "Structure of Velocity Space-Time Correlations in a Boundary Layer," *The Physics of Fluids Supplement*, 1967, pp. S138–S145.

[8] Owen, F. K., "Transition Experiments on a Flat Plate at Subsonic and Supersonic Speeds," *AIAA Journal*, Vol. 8, No. 3, March 1970, pp. 518–523.

[9] Dhawan, S. and Narashima, R., "Some Properties of Boundary Layer Flow during the Transition from Laminar to Turbulent Motion," *Journal of Fluid Mechanics*, Vol. 3, 1958, pp. 418–436.

[10] Dwyer, H. A., Doss, E. D., and Goldman, A. L., "A Computer Program for the Calculation of Laminar and Turbulent Boundary Layer Flows," CR-114366, 1971, NASA.

[11] Owen, F. K. and Horstman, C. C., "A Study of Turbulence Generation in a Hypersonic Boundary Layer," AIAA Paper 72-182, San Diego, Calif., 1972.

[12] Kline, S., Reynolds, W., Schraub, F., and Runstadler, P., "The Structure of Turbulent Boundary Layers," *Journal of Fluid Mechanics*, Vol. 30, 1967, pp. 741–773.

[13] Laufer, J., "Some Statistical Properties of the Pressure Field Radiated by a Turbulent Boundary Layer," *The Physics of Fluids*, Vol. 7, No. 8, 1964, pp. 1191–1197.